1987

Shoreward Intrusion of Upper Gulf Stream Water onto the United States Southeastern Continental Shelf

Lie-Yauw Oey
Old Dominion University

Larry P. Atkinson
Old Dominion University, latkinso@odu.edu

Jackson O. Blanton

Original Publication Citation

Oey, L.Y., Atkinson, L.P., & Blanton, J.O. (1987). Shoreward intrusion of upper gulf stream water onto the United States southeastern continental shelf. *Journal of Physical Oceanography, 17*(12), 2318-2333. doi: 10.1175/1520-0485(1987)0172.0.co;2

Shoreward Intrusion of Upper Gulf Stream Water onto the U.S. Southeastern Continental Shelf

LIE-YAUW OEY AND LARRY P. ATKINSON

Department of Oceanography, Old Dominion University, Norfolk, VA 23508

JACKSON O. BLANTON

Skidaway Institute of Oceanography, Savannah, GA 31416

(Manuscript received 24 April 1987, in final form 7 July 1987)

ABSTRACT

In winter, cooling of the South Atlantic Bight continental shelf water results in higher density in the middle shelf region relative to the shelf-break region where the western flank of the Gulf Stream flows. Shoreward, estuarine-like intrusion of the upper Gulf Stream water in the presence of such a positive onshore density gradient is then possible through advective processes triggered either by the meander of the Stream or onshore Ekman transports by southward wind stresses. Repeated cross-shelf hydrographic transects were conducted from 10 January through 30 January 1986 to more closely study this intrusion process. These observations show many features predicted by a previous numerical model study. A semi-empirical model is proposed here wherein the state of stratification of water on the outer continental shelf region just inshore of the shelf break is used as an indicator of the intrusion process. Model analysis suggests correlating the observed time rate of change of potential energy of the water column with wind-induced cross-shelf Ekman transport. The correlation fit is good for at least half of the dataset, suggesting that wind-induced intrusion was significant during the observations. The analysis also suggests that it is possible to distinguish intrusion processes which are wind induced from those which are induced by Gulf Stream meanders.

Both observations and the previous numerical model study show transient shelf-break upwelling following a southward wind impulse. A simplified model suggests that the upwelling is a result of a cyclonic vortex, bounded at the shelf break, produced by interaction of wind stress and sloping bottom topography. Transient upwellings introduce Gulf Stream water from below the mixed layer to the sea surface, where it is transported onshore to the continental shelf by intrusion processes. This provides a mechanism by which nutrient-rich, deeper Gulf Stream water can replenish the water mass of the adjacent continental shelf.

1. Introduction

Oey (1986, henceforth O86) discussed the possibility that during winter in the South Atlantic Bight (SAB), strong southward (henceforth the term "southward" is used in a general sense to denote a direction which is against the north-northeastward flow of the Gulf Stream) wind stress can transport upper (~50 m) Gulf Stream water shoreward onto the continental shelf, and that continental shelf fronts form when the warm Gulf Stream water mixes with cooler shelf water. Working hypotheses which describe these intrusion and mixing processes are

1) Strong wintertime wind stress (~2 dyn cm^{-2}) and cold, dry continental air produce an upper mixed-layer depth of O(100 m). As a result, shelf water is vertically well mixed and the "western wall" of the Gulf Stream front surfaces to form a front at the shelf break (Fig. 1a). The cold wind induces heat and mass losses from the ocean's surface and continuously cools the shelf waters. The temperature of Gulf Stream water, however, remains essentially unchanged because of a continuous replenishment of warm water from the south. Thus, the shelf break front separates warm upper Gulf Stream water from cooler shelf water.

2) Strong southward wind impulses of about 10 dyn cm^{-2} day can break down the shelf-break front. Warm Gulf Stream water then spills onto the continental shelf where it mixes with cooler shelf water to produce frontal zones (Fig. 1b).

3) Continental shelf fronts, once formed, must be maintained by southward wind stresses which continuously introduce warmer offshore water converging at the front. The wind also induces downward turbulent diffusion of heat which balances the downwelling (weakening), seaward advection of cold water at the foot of the front (Fig. 1c).

A two-dimensional (cross shelf and depth), time-dependent numerical model which calculates vertical mixing processes via the turbulence energy and length-scale equations was used in O86 to test the hypotheses. Model results show the importance of (i) density gradients across the shelf break and the outer continental

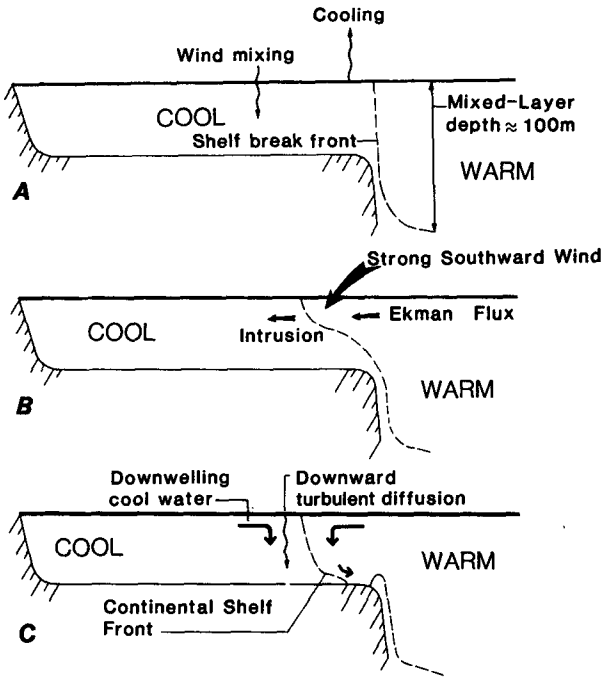

FIG. 1. A schematic sketch of the shoreward intrusion of upper Gulf Stream water as a result of southward wind forcing in winter, and the subsequent formation of continental shelf front.

the dynamics and thermodynamics of the intrusion process.

Oey's numerical model study is somewhat hypothetical since no attempt was made to simulate any particular intrusion event. While model results are valuable in guiding us to perceive our hypotheses and design of the field experiment, they cannot be directly used to correlate observations. In this paper, we give a simpler model which incorporates the essential elements contained in the more complicated version presented in O86. It is possible then to express the significant flow dynamics and thermodynamics in a semi-empirical relation containing a few parameters which can be calculated from observations. In this way we are able to separate, approximately, shoreward intrusion events which are wind-induced from those which are caused by Gulf Stream meanders and frontal eddies.

The organization of this paper is as follows: section 2 will present observational data. Section 3 gives formulation of the simplified model of intrusion processes, and in section 4 model relationships between stratification, wind work and wind-induced advection are used to correlate observed data. In section 5 we present a simple model which describes the shelf-break upwelling following a southward wind event, seen in field observations, as well as in Oey's model results. Section 6 contains discussions of our result and its implication

shelf; (ii) onshore/offshore Ekman transports by alongstream wind stresses and (iii) vertical mixing by winds in the proposed dynamics and thermodynamics of frontal intrusion processes. It is important to recognize the dual role played by the wind stress which, on one hand, produces stratification in the water column by inducing advection in the presence of horizontal density gradients and, on the other hand, homogenizes the water column through work at the water surface (Fig. 1). Oey also mentions that the first role—advection in the presence of a density gradient—can be due to mechanisms other than the winds. He suggests shoreward intrusion due to Gulf Stream meanders and frontal eddies as being a plausible mechanism.

Some temporal "snapshots" of hydrographies across the outer shelf and shelf break were presented in O86 to illustrate the intrusion process. Due to the short temporal coverage, these data do not give direct and convincing demonstration of the hypotheses. As part of the oceanographic component of Project GALE (Genesis of Atlantic Low Experiment), we proposed to test these hypotheses by making repeated hydrographic measurements along a cross-shelf transect off Charleston, South Carolina (Fig. 2). The measurements were taken from 10 January through 30 January 1986, at time intervals of approximately 1–3 days. Together with meteorological data from an offshore buoy station, the temporal and spatial structure of the measured distribution make it possible to examine quantitatively

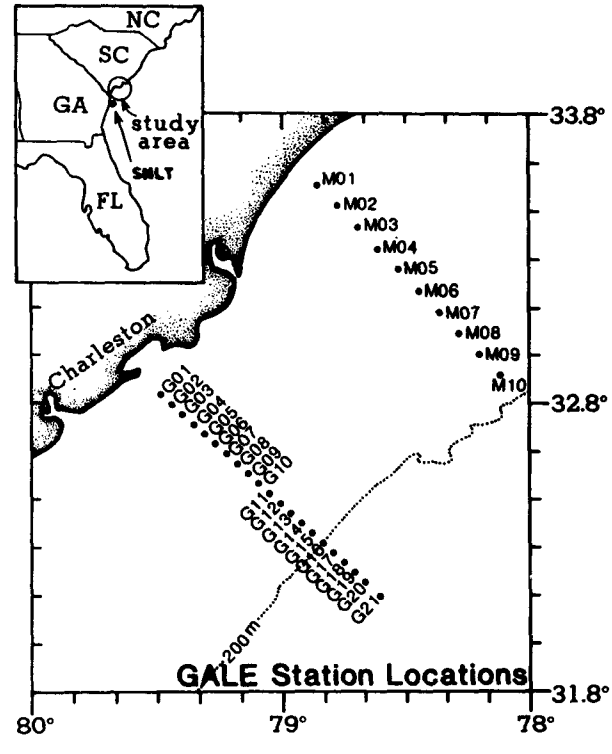

FIG. 2. Location map of GALE transects off Charleston and Myrtle Beach. Most of the hydrographic measurements were taken at the Charleston transect and these are the results discussed in the text. SNLT denotes Savannah Navigation Light Tower.

to wintertime water mass renewal in the outer-shelf region of the SAB. The paper concludes with section 7.

2. Observational results

Figure 2 shows the two cross-shelf transects where hydrographic measurements were taken on board the *Endeavor* from 10 January through 30 January 1986. About 80% of the observations were conducted at the Charleston transect; these are the results which we will discuss and use here. (Details of the cruise are given in the report by Atkinson et al., 1986). Meteorological data for the month of January, measured at the Savannah Navigation Light Tower (SNLT, 32°N, 80.7°W approximately 30 km offshore of Savannah at the 15 m isobath), are shown in Fig. 3. The wind stress vectors have been rotated to correspond approximately to the alongshelf and cross-shelf directions (i.e., approximately in the along-Stream and cross-Stream directions, respectively). Cycles of strong northeasterly and west-northwesterly winds are seen to be associated with cold air outbreaks and rising barometric pressures preceded by atmospheric lows. The period of these weather cycles is about 5–10 days, consistent with what is known about the wind energetics in the SAB during winter (e.g., Brooks and Bane, 1983). The more prominent "weather events" occurred on 8–12, 21–24 and 26–28 January (Fig. 3).

The temperature, salinity and σ_t contours across the transect are presented in Figs. 4–6. These show a number of features which are worth noting. First, significant cross-shelf salinity variations are confined within a nearshore band from the coast to about the midcontinental shelf region at approximately the 30 m isobath. This reflects some coastal "freshening" due to river discharges along the coasts of South Carolina and Georgia. Water temperatures in the inner shelf region are cooler than those further offshore in the midshelf, a consequence of faster "local" cooling of the shallower water. A good first approximation to the dynamics and thermodynamics of this nearshore band is therefore obtained by assuming that it is effectively "sheltered" from influences of the outer-shelf water. A one-dimensional model in the vertical which accounts for heat exchanges across the air–sea interface is sufficient to determine its heat content (O86). In this nearshore band, the temperature and salinity compensate somewhat in determining the density variation. By and large, however, the salinity effect is dominant and density increases steadily from the coast to the mid-shelf region.

Beyond the 30 m isobath in the outer continental shelf and shelf break regions salinity variation is insignificant and density variations are determined by temperature variations. Hence density decreases in the offshore direction and, together with an increase in density from coast to the midshelf, a density maximum is often found in the mid-shelf region around the 30 m isobath (Figure 6).

Finally, the temperature and σ_t plots in the outer-shelf and shelf-break regions often show shoreward intrusion of the upper mixed layer of warm Gulf Stream water. Intrusion starts at the shelf break where the upper 50 m or so of the isotherms/isopycnals tilt shoreward. This is most clearly seen on 12 and 30 January. The latter event is most likely Gulf Stream meander induced, as winds on and prior to 30 January are west-southwesterly. This wind condition is consistent only with an offshore Ekman transport, not with the onshore intrusion, as observed (Figs. 4k and 6j). The event on 12 January (Figs. 4b and 6b) coincides with a strong southward wind event and has many features which are consistent with our hypotheses set forth in the Introduction. It is useful, therefore, to first discuss this event in purely descriptive terms and relate qualitatively observations with Oey's numerical model results. In section 3, we will formulate a simplified model that incorporates the essential mechanics of the intrusion process, and that can be used in a quantitative correlation of the observed data.

a. Establishment of a "shelf-break front"

Due to repeated invasions of cold air and strong winds during the late autumn and early winter months, shelf water cooled and became vertically well mixed. The depth of the mixed layer over the Gulf Stream was about 50–100 m and a shelf-break front was established (Figs. 4 and 6).

b. Shoreward intrusion

On 8 January 1986, wind started to pick up from the north-northeast, reached a maximum of about 10 m s^{-1} and remained essentially unchanged in direction through 12 January (Fig. 3). These conditions favor the shoreward intrusion of Gulf Stream water. Temperature and σ_t contours from 10 January (Figs. 4a and 6a) through 14 January (Figs. 4c and 6c) illustrate the response of upper Gulf Stream and continental shelf waters to this wind event. At the time the first hydrographic transect was taken, shoreward Ekman transport of the upper Gulf Stream water had begun, as evidenced by the shoreward tilt in the upper part of temperature (and σ_t) contours (Figs. 4a and 6a). By 12–13 January (Figs. 4b and 6b) the upper portion of the shelf-break front moved shoreward and warm water intruded onto the continental shelf. For example, the 19°C isotherm moved onshore about 10 km, a distance which is approximately equal to a velocity of 6 cm s^{-1} over a 2 day time period. The average onshore velocity is consistent with the averaged wind-induced Ekman velocity $= \tau_0^y/(\rho_0 fh)$, where the kinematic alongstream wind stress $\tau_0^y/\rho_0 \approx 3 \times 10^{-4}$ m^2 s^{-2}, the Coriolis parameter $f \approx 10^{-4}$ s^{-1} and the water depth $h \approx 50$ m.

The formation of a continental shelf thermal front at about the 30 m isobath was brought about by the mixing of intruded warm water with the cooler shelf

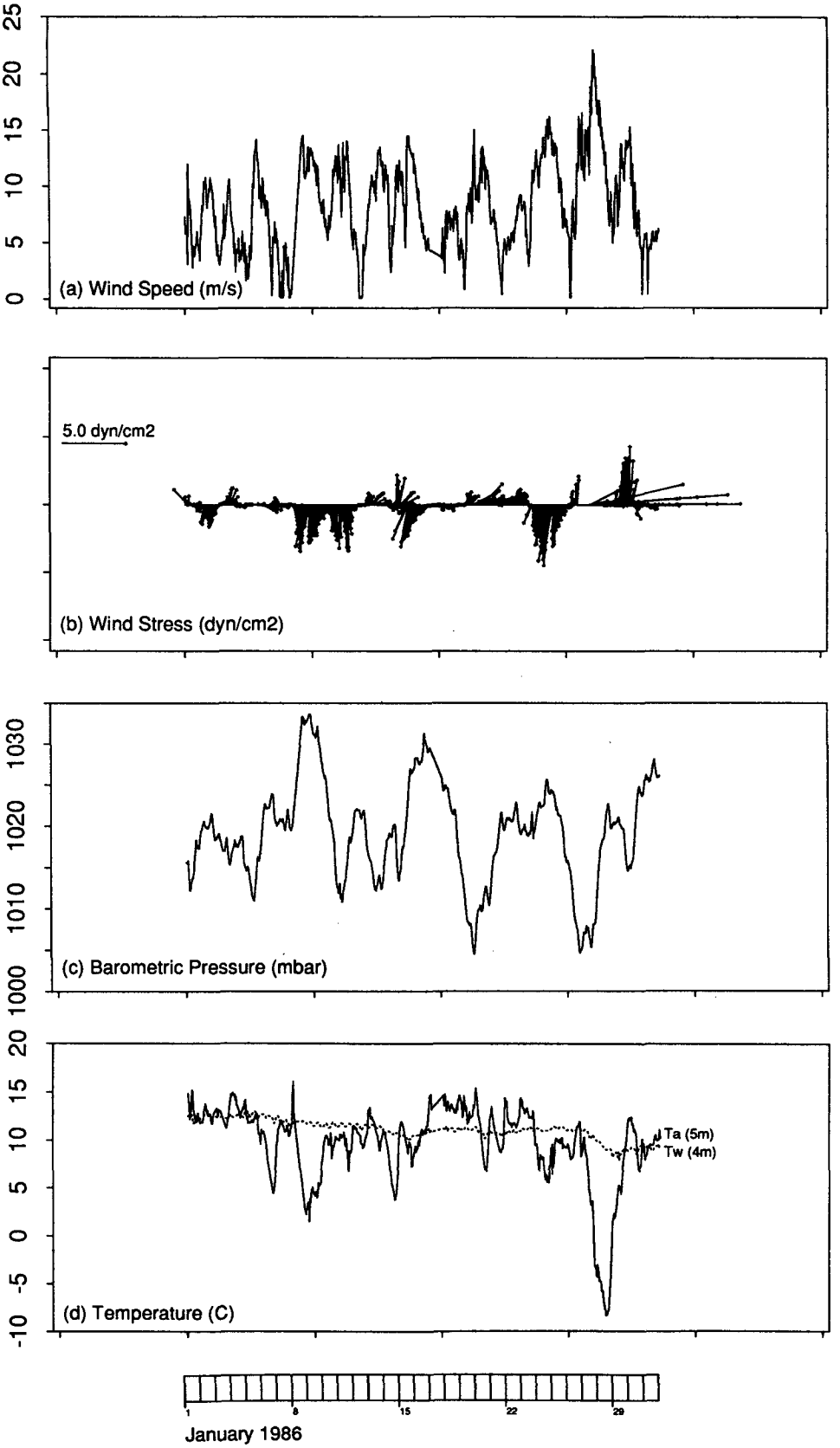

FIG. 3. SNLT meteorological data. Shown are (a) wind speed (m s^{-1}), (b) rotated wind stress vector (dyn cm^{-2}), (c) barometric pressure (mbar), and (d) air temperature at 5 m above the sea-surface and water temperature at 4 m below the sea surface.

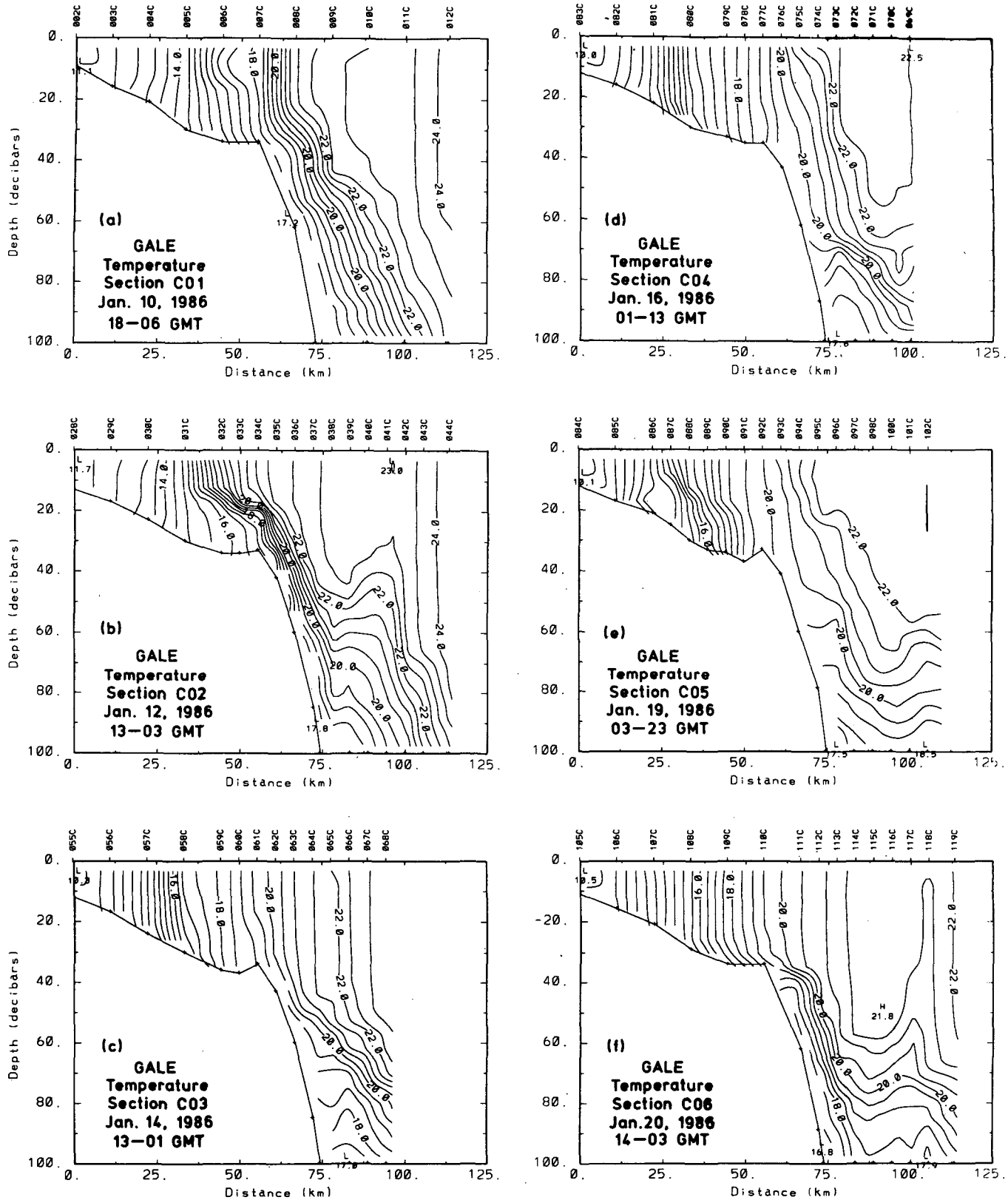

FIG. 4. Temperature (°C) contours (CI = 0.5°C) at the Charleston transect from 10–30 January 1986. 25 January had XBT casts only.

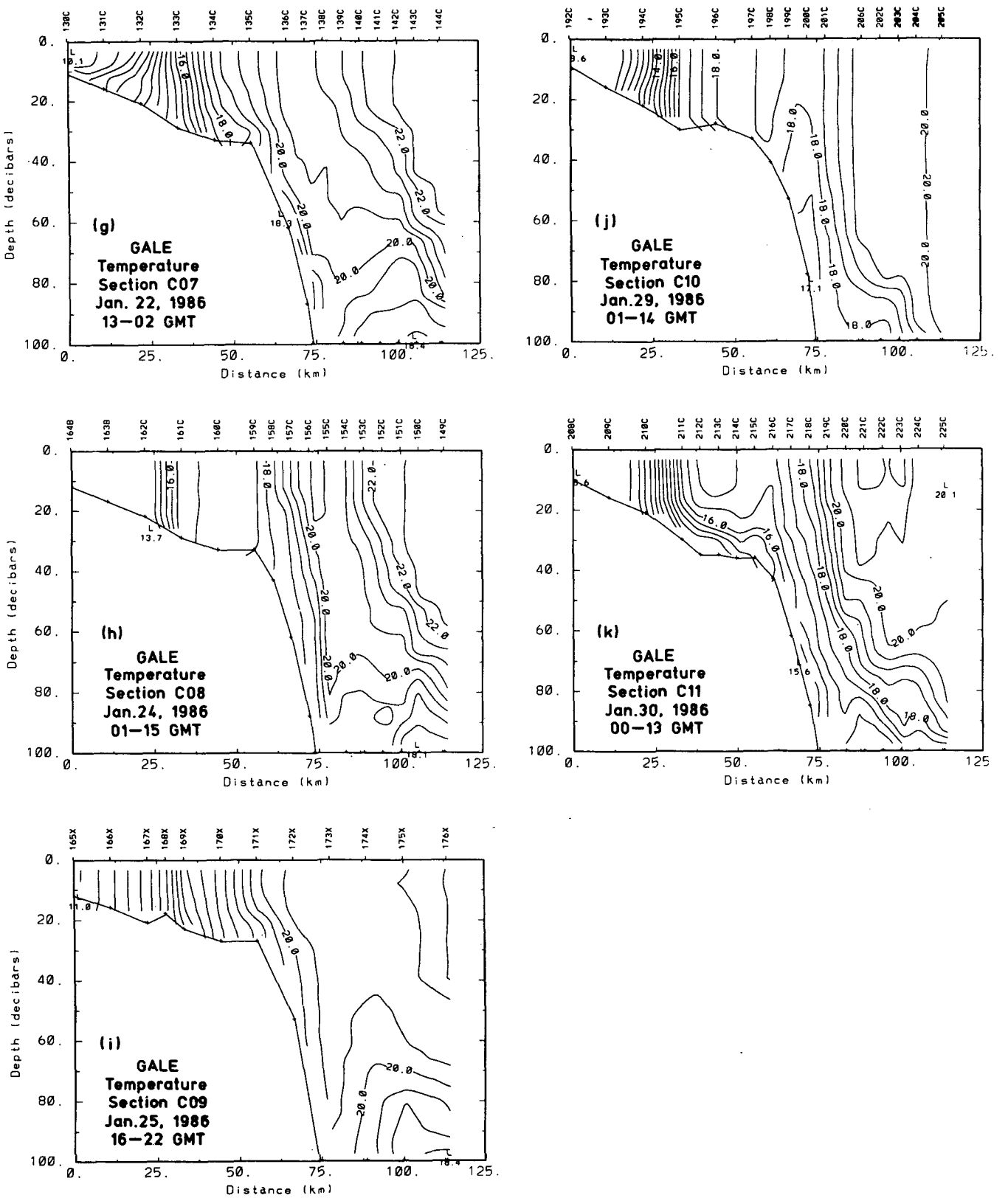

FIG. 4. (*Continued*)

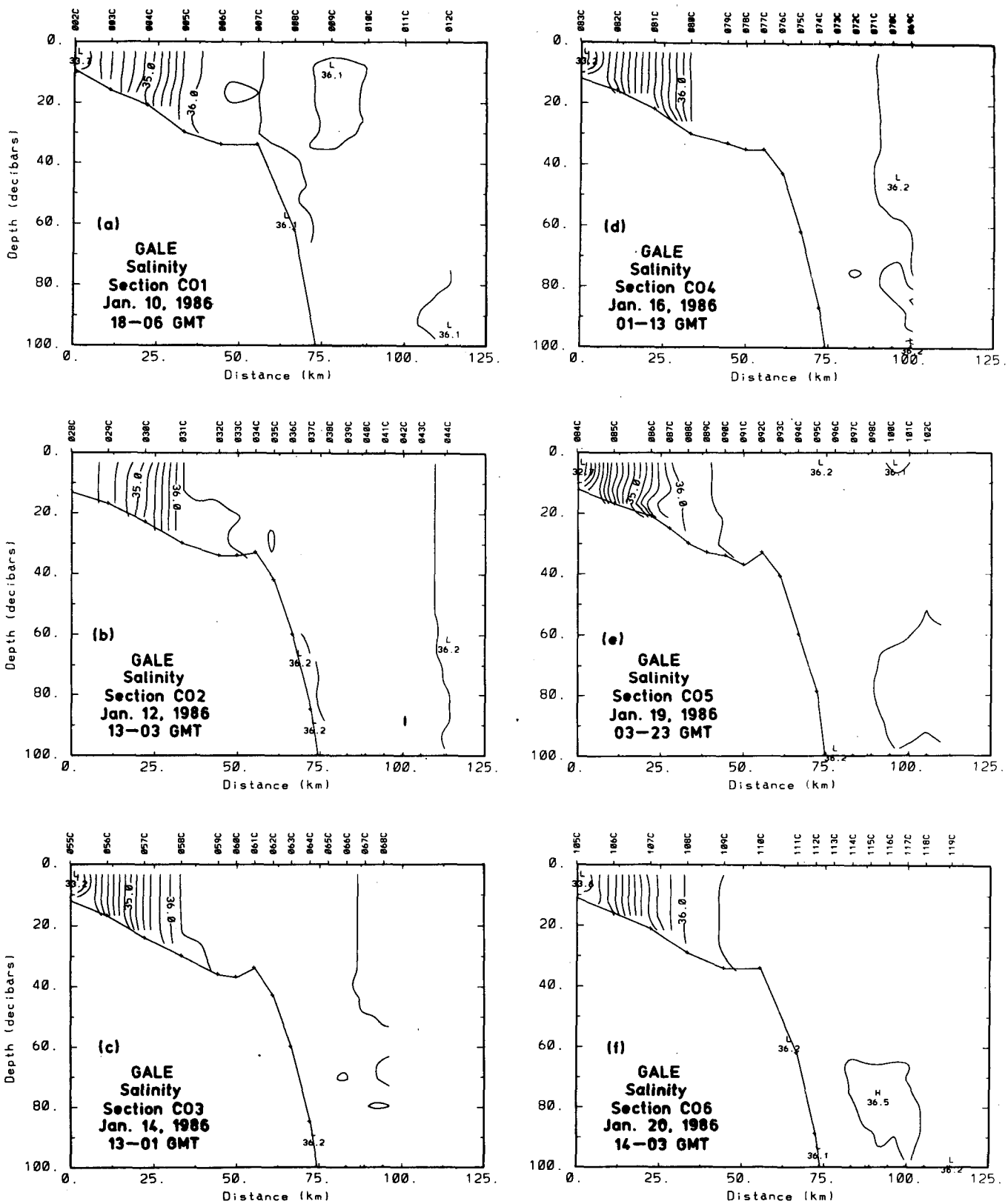

FIG. 5. As in Fig. 4 but for salinity (‰; *CI* = 0.2‰).

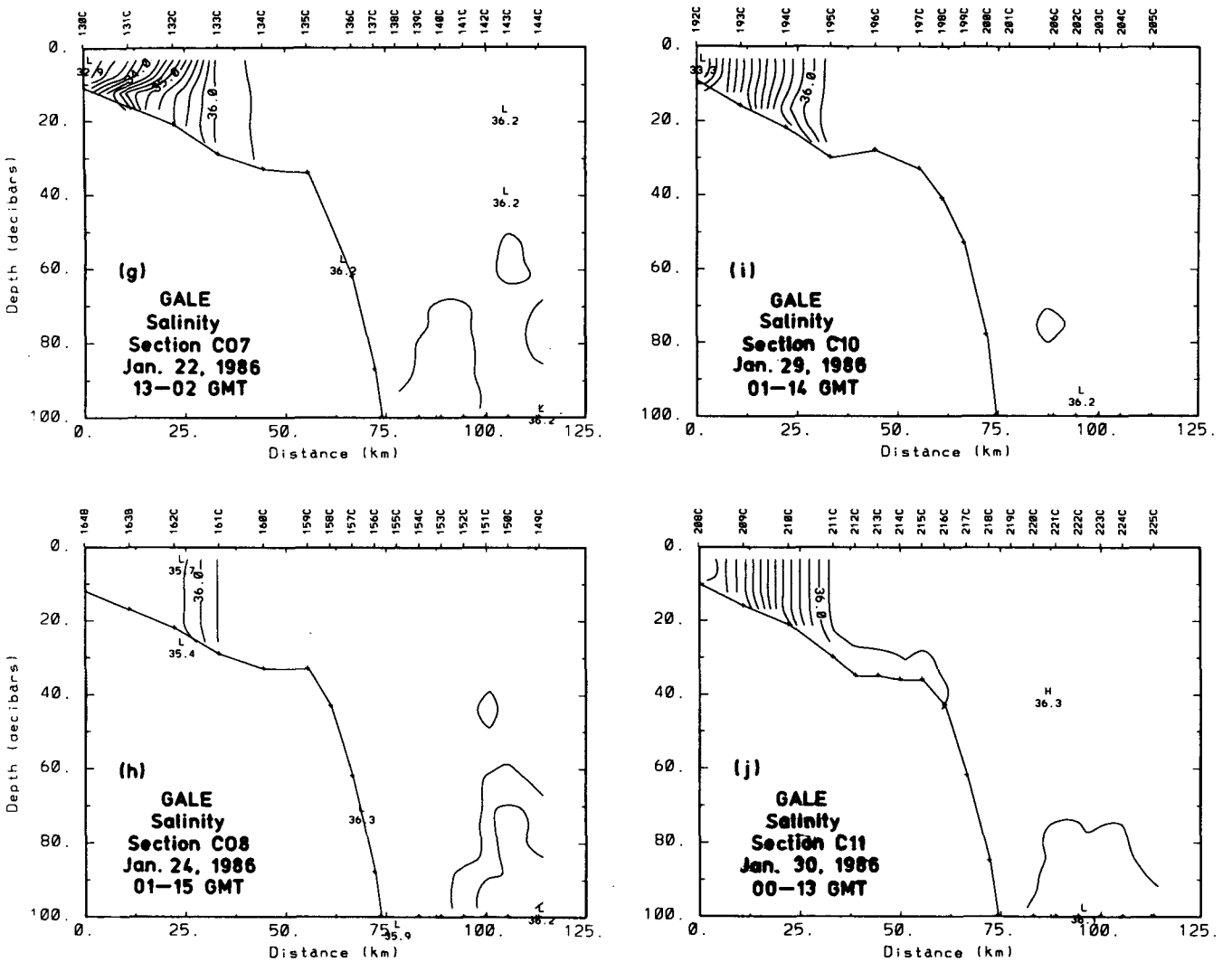

FIG. 5. (*Continued*)

waters (Fig. 4b). There also appears to be a region of upwelling over the shelf break and continental slope. This pattern, the formation of a continental shelf thermal front and upwelling over the shelf break, is consistent with Oey's (1986) computed isopycnals and cross-shelf circulation patterns (Fig. 7; taken from his Fig. 11c). The figure shows results from Oey's model one day after a southward wind impulse ($\sim$4 dyn cm^{-2} over 4 days) has stopped. The wind impulse used in the model is close to that observed, $\sim$3 dyn cm^{-2} over 4 days, and Fig. 4b corresponds to a relaxation response after the wind ceased. Apart from measured σ_t values, which differ from those used in the model because of differences in initial values, other features, including the onshore movement of the upper portion of the shelf-break front, the upwelling region over the shelf-break/slope region, and the formation of a lens of warm (less dense) water just above the upwelled water, are reproduced rather well by the model. The model suggests a cross-shelf circulation pattern as follows: warm upper Gulf Stream water converges with cooler water over the continental shelf and there is downwelling at the foot of the front. This downwelling advects cooler water to the shelf break and slope regions. Part of the downwelled water is eventually entrained in the upwelled water over the shelf break. Divergent flow occurs above the upwelling region over the shelf break/slope. This circulation pattern is shown schematically in Fig. 8.

c. *Wind mixing after intrusion*

After a brief relaxation on 12 January, winds strengthened ($\approx$2 dyn cm^{-2}) between 13 and 15 January and were generally from the west (Fig. 3). The effect of wind mixing on the continental shelf front,

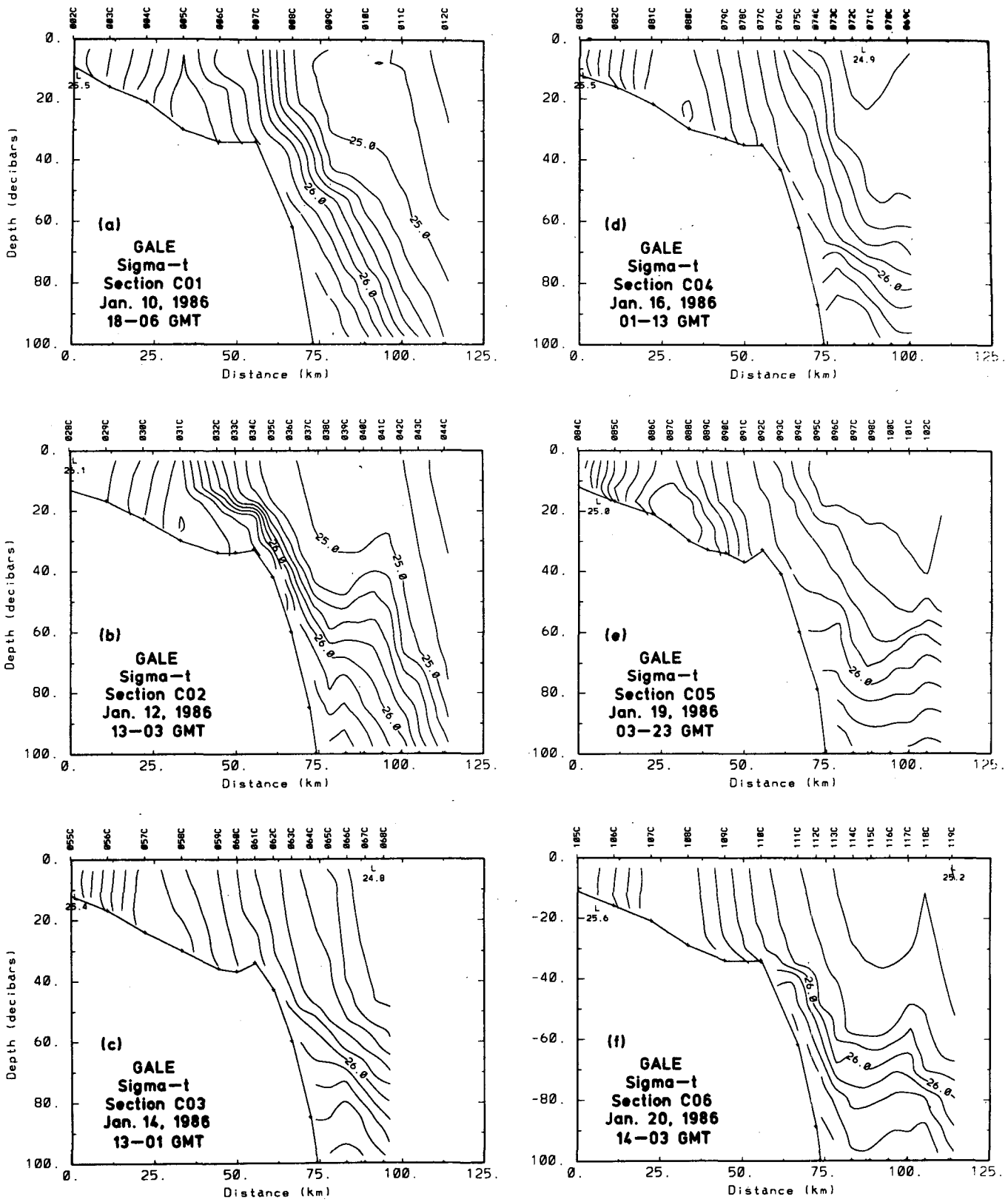

FIG. 6. As in Fig. 4 but for density in σ_t values (kg m^{-3}; CI = 0.2 kg m^{-3}).

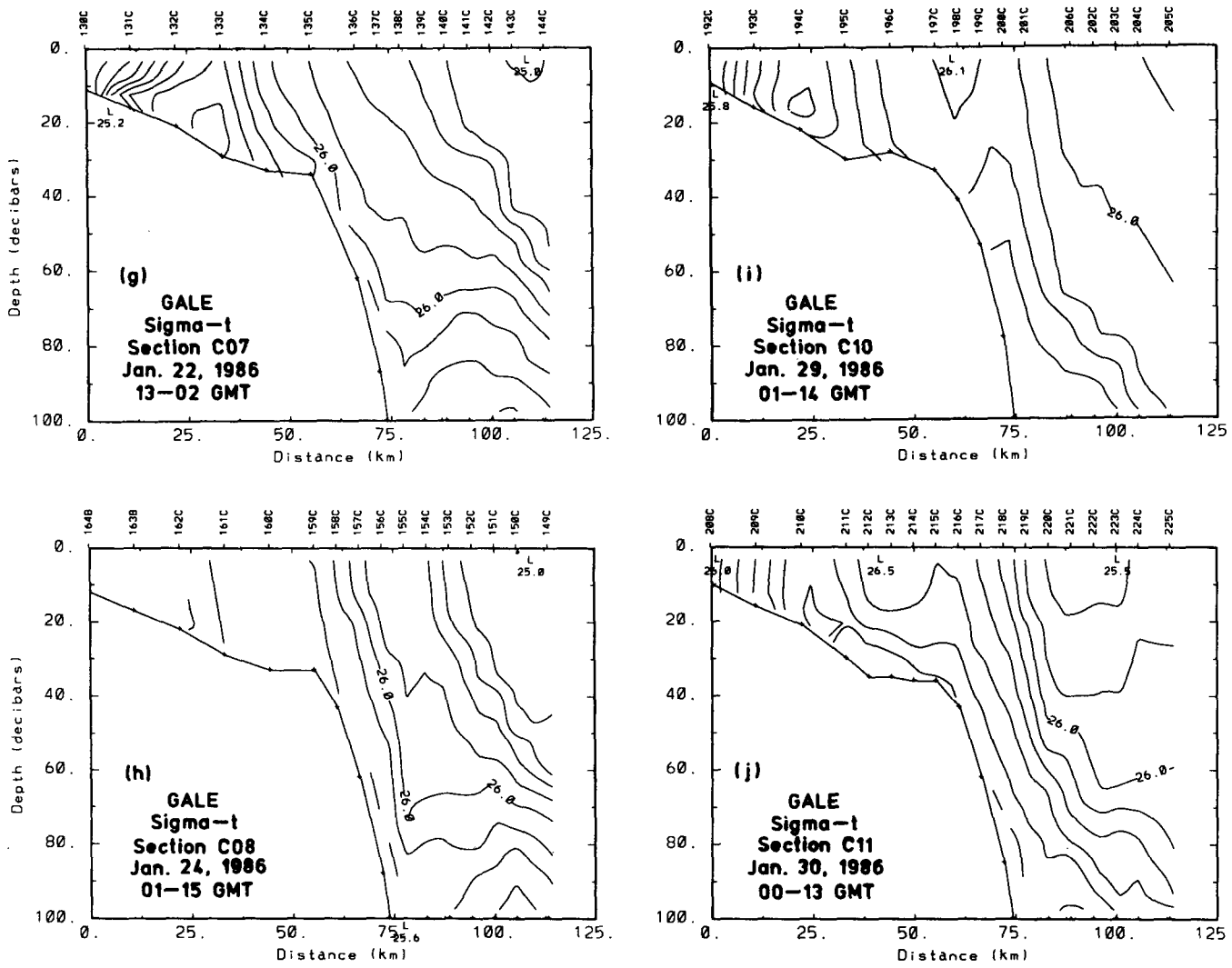

FIG. 6. (*Continued*)

according to hypothesis 3, is to cause downward turbulent diffusion of heat, which homogenizes the water column and reduces the tilt of the front. Figure 4c shows, for example, that the previously inclined 18°C isotherm (Fig. 4b) has now become vertical. The front weakened somewhat, however, because: (i) generally offshore wind introduced low-salinity water to the front and lowered the density of water on the shoreward side of the front; and (ii) wind-induced Ekman flux is offshore and southward rather than onshore; thus, there is no new supply of warm water, and convergence at the front weakens. Note also that the cold dome caused by upwelling over the shelf break/slope region has nearly disappeared, indicating its short-period, transient nature.

d. The next event

On 15–19 January there was a brief episode of northeasterly wind. Again there was evidence of onshore transport of upper Gulf Stream water in the mixed layer (Figs. 4d, e and 6d, e).

3. A model of the intrusion process

Our aim is to formulate a semi-empirical model which will take into account the essential features of the intrusion process seen in the observations. The model will serve as a gross skeleton of Oey's (1986) numerical model; being simplified, its parameters can be calculated from field data. Thus, a direct quantitative comparison of model results (and our hypotheses) with observations can be made and one can subsequently assess the importance of wind-induced versus Gulf Stream meander-induced intrusions.

As stated earlier, the model must incorporate three physical elements: (i) cross-shelf density gradient ρ_x in the outer shelf to shelf-break regions, (ii) onshore/offshore Ekman transports by alongstream wind stresses

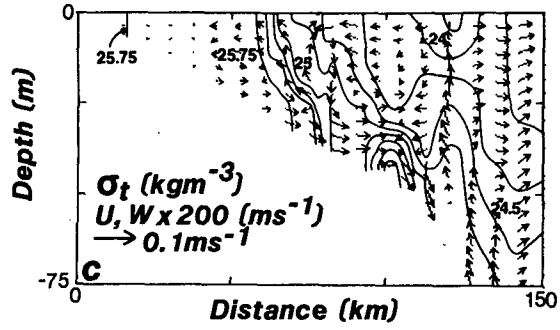

FIG. 7. Numerical model results one day after a southward wind forcing event, which lasted for about 4 days, has stopped. The figure shows the initial formation of a continental shelf front on the 30 m isobath and the upward doming of isopycnals at the shelf break (after Oey, 1986).

and (iii) vertical mixing by winds. In subsequent analyses, the horizontal axes (x, y) lie on the mean sea surface where $z = 0$, x and y are positive offshore and "northward" (i.e., in the flow direction of the Gulf Stream) respectively, and z is positive upward; the subscripts x, y, z and t (time) on dependent variables such as the density ρ will denote partial derivatives. Here ρ_x will be treated as given and, analogous to steady-state calculations of density distributions in estuaries (e.g., see Oey, 1984), will be assumed to be a function of x only. Thus, we set

$$\rho_x = d\langle\rho\rangle/dx \tag{1}$$

where the angle brackets denote vertical averaging over the water column of depth h:

$$\langle\rho\rangle = \int_{-h}^{0} \rho dz/h. \tag{2}$$

The $d\langle\rho\rangle/dx$ can be viewed as a "background" quantity, the temporal scale of which is long in comparison with the time scales of occurrences of weather events and Gulf Stream meanders. This simplifying assumption will be checked a posteriori.

As in O86, it is assumed that the motion is in the cross-shore and depth (two-dimensional) plane, so that all y-derivatives are dropped. Thus, the essence of the intrusion process is taken to be cross-shelf advection (induced by winds and/or Gulf Stream meanders) in the presence of a background cross-shelf density gradient, modified by vertical mixing due to winds, tides, and density overturnings.

As an indicative index of intrusion, we use Simpson and Hunter's (1974) definition of potential energy

$$\mathrm{PE} = \int_{-h}^{0} [\rho - \langle\rho\rangle] gz dz, \tag{3}$$

calculated in the outer-shelf region. Therefore, PE measures the state of stratification in the outer shelf and, if decreased, would indicate shoreward intrusion (Fig. 6 and O86). Note that observations show stratification in the outer shelf whenever there is a shoreward intrusion, irrespective of whether the intrusion is wind induced (as in Figs. 4b, 6b) or Gulf Stream meander-induced (as in Figs. 4k, 6j).

The following analysis follows van Aken's (1985) extension of Simpson and Hunter's (1974) model of stratification. The density of a fluid parcel satisfies [Eq. (5) in O86]:

$$\rho_t = -(\overline{w'\rho'})_z - \mathbf{u}\cdot\nabla\rho \tag{4}$$

where the primes denote turbulent fluctuations, $\mathbf{u} = (u, v, w)$ is the ensemble mean velocity vector and the overbar denotes an ensemble mean. With the assumption that

$$\nabla\rho = (d\langle\rho\rangle/dx, 0, 0) \tag{5}$$

we have

$$\mathbf{u}\cdot\nabla\rho = (\langle u\rangle + \hat{u}) d\langle\rho\rangle/dx, \tag{6}$$

where the cross-shelf velocity component u is split into two parts: 1) a depth-averaged part $\langle u\rangle$ and 2) a part $\hat{u}$ which represents deviation from $\langle u\rangle$. Substitution of (4), (5) and (6) into the time derivative of (3) gives

$$(\mathrm{PE})_t = g\int_{-h}^{0} \overline{w'\rho'} dz - (gh/2)\overline{w'\rho'}|_0 - \mathrm{g}d\langle\rho\rangle/dx \int_{-h}^{0} \hat{u} z dz. \tag{7}$$

The first term on the rhs of (7) represents vertical turbulent mixing of layered waters of different densities and can be related to wind and tidal work as follows. The equation for the turbulence kinetic energy q^2 is (Mellor and Yamada, 1974; Eq. (9) of O86)

$$(q^2/2)_t + \mathbf{u}\cdot\nabla(q^2/2) = [K(q^2/2)_z]_z - \overline{u'w'}u_z - \overline{v'w'}v_z - \rho_0^{-1}\overline{gw'\rho'} - q^3/l \tag{8}$$

where "K" is the vertical diffusion coefficient for q^2 and l is a length scale. The first term on the rhs of (8) is a parameterization of the triple correlation of velocity

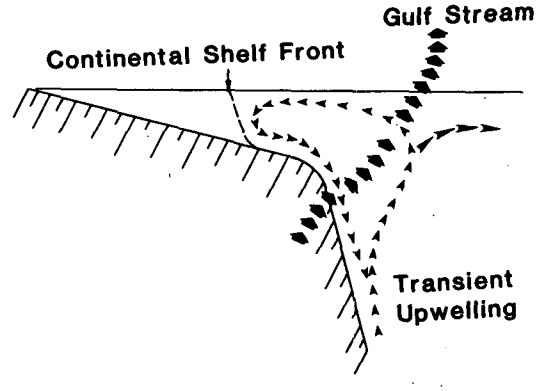

FIG. 8. A schematic sketch of transient, wind-induced upwelling processes inferred from observations and numerical model results.

fluctuations which effectively acts to redistribute turbulence kinetic energy in the water column. The second and third terms are shear productions, while the fourth term is the buoyancy production term. The last term parameterizes viscous dissipation due to small-scale velocity fluctuations. Assuming (i) a level-one turbulence model (Mellor and Yamada, 1974) which effectively sets the lhs of (8) to zero; (ii) $l \approx h$ and $q \approx (|\tau|/\rho_0)^{1/2}$, where τ is a boundary stress vector (either at the sea surface or near the bottom) and ρ_0 is a reference density; and (iii) quadratic stress laws for wind and bottom stresses, τ_0 and τ_b, one obtains from a vertical integration of (8):

$$g\int_{-h}^{0}\overline{w'\rho'}dz \approx \rho_a C_{0a} C_a|\mathbf{u}_a|^3 + \rho_0 C_{0b} C_b|\mathbf{u}_T|^3 \qquad (9)$$

where $\mathbf{u}_a = (u_a, v_a)$ is the wind velocity vector, $\mathbf{u}_T = (u_T, v_T)$ is the tidal velocity vector, C_a and C_b are the wind and bottom drag coefficients, respectively, with values of about 2×10^{-3}, $C_{0a} \approx |\mathbf{u}(x, y, z = 0, t)|/|\mathbf{u}_a|$, $C_{0b} \approx |\mathbf{u}(x, y, z = -h, t)|/|\mathbf{u}_T|$ and ρ_a is the density of air.

The second term on the rhs of (7) can be simply related to heat and salt fluxes across the air–sea interface if one assumes linear dependency of ρ' to T' and S', where T' and S' are the temperature (in °C) and salinity (in ‰) fluctuations, respectively,

$$\rho'/\rho_0 = -\alpha T' + \beta S' \qquad (10)$$

where

$$\alpha = -(\partial\rho/\partial T)/\rho \approx 2\times 10^{-4}\,\mathrm{K}^{-1}$$

$$\beta = (\partial\rho/\partial S)/\rho \approx 8\times 10^{-4}$$

and the approximate values of α and β are taken from Gill (1982). Then,

$$-\overline{w'\rho'}|_0 = \alpha Q/C_{pw} + \beta S_0(E_v - P_r) \qquad (11)$$

where

Q total heat flux across the air–sea interface in W m^{-2}, positive upward;
C_{pw} specific heat of water at constant pressure $\approx 4 \times 10^3$ J kg^{-1} K^{-1} (Gill, 1982);
S_0 near-surface ocean salinity in ‰;
$(E_v - P_r)$ rate of evaporation minus precipitation in kg m^{-2} s^{-1}.

The third term on the rhs of (7) is the differential advective term in the presence of a cross-shelf density gradient. To evaluate this term we note that cross-shelf transport $\langle u\rangle$ is ≈ 0 because the continental-shelf front acts effectively as a dynamic barrier separating the inner-shelf and outer-shelf waters and significant transports occur only in the alongfront direction (see O86). Thus, onshore transport in the upper Ekman layer of depth $D \approx 0.1(|\tau_0|/\rho_0)^{1/2}/f$ must be compensated by a corresponding offshore transport in the lower layer. With a "typical" average alongstream wind stress in Fig. 3 of about 1–2 dyn cm^{-2} (0.1–0.2 N m^{-2}), $D \approx$ 10–20 m in outer-shelf waters of depths 30–40 m. This gross pattern of cross-shelf circulation can be seen in Oey's model results. Thus, since the integral moment of the velocity deviation, $\int_{-h}^{0}\hat{u}z dz$, is not expected to be particularly sensitive to the form of $\hat{u}$, we use the simple form:

$$\hat{u} = 2\tau_0^y/fh\rho_0, \quad -h/2 \leqslant z \leqslant 0$$
$$-2\tau_0^y/fh\rho_0, \quad -h \leqslant z < -h/2. \qquad (12)$$

Other more sophisticated forms with linear or even polynomial variation could perhaps be used. This would not be justifiable, however, given that other gross simplications have already been built into the model.

With (9), (11) and (12), Eq. (7) becomes

$$(\mathrm{PE})_t = \rho_a C_{0a} C_a|\mathbf{u}_a|^3 + \rho_0 C_{0b} C_b|\mathbf{u}_T|^3 + (gh/2)[\alpha Q/C_{pw} + \beta S_0(E_v - P_r)] - gd\langle\rho\rangle/dx\tau_0^y h/(2f\rho_0). \qquad (13)$$

Thus, wind and tidal work, surface cooling (positive Q), evaporation, and northward wind stress ($\tau_0^y > 0$) in the presence of negative $d\langle\rho\rangle/dx$ all tend to increase PE and hence vertical mixing. Surface warming (negative Q), precipitation, and southward wind stress ($\tau_0^y < 0$) all tend to decrease PE and hence induce stratification.

4. Correlating observations

By dividing (13) through by the wind and tidal work terms we obtain the following nondimensionalized relation

$$(\mathrm{PE})_t/M = 1 + (gh/2)[\alpha Q/C_{pw} + \beta S_0(E_v - P_r)]/M - d\langle\rho\rangle/dx(gh)^{1/2}/(2\rho_0 f)[(gh)^{1/2}\tau_0^y/M], \qquad (14)$$

where

$$M = \rho_a C_{0a} C_a|\mathbf{u}_a|^3 + \rho_0 C_{0b} C_b|\mathbf{u}_T|^3.$$

Thus, if the surface flux term [the second term on the rhs of (14)] is slowly varying in time over a wind cycle of five to ten days, one can assess from (14) the importance of wind-induced intrusion by monitoring from observations the change in PE. Equation (14) can then be rewritten as

$$Y = C_1 + C_2 X, \qquad (15a)$$

where

$$Y = (\mathrm{PE})_t/M$$

$$X = (gh)^{1/2}\tau_0^y/M$$

$$C_1 = 1 + (gh/2)[\alpha Q/C_{pw} + \beta S_0(E_v - P_r)]/M$$

$$C_2 = -d\langle\rho\rangle/dx(gh)^{1/2}/(2\rho_0 f),$$

which is a linear correlation equation relating the rate of change of the state of stratification of the water column, Y, to the wind-induced intrusion parameter, X. If $|\mathbf{u}_a|$ is nonzero, we can instead divide (13) by $\rho_a C_a|\mathbf{u}_a|^3$. Since the tidal work term is also expected to be slowly

varying in time, Eq. (15a) remains valid with C_1 and M now redefined to be, respectively,

$$C_1 = C_{0a} + \rho_0 C_{0b} C_b |\mathbf{u}_T|^3/M + (gh/2)[\alpha Q/C_{pw} + \beta S_0(E_v - P_r)]/M,$$

$$M = \rho_a C_a |\mathbf{u}_a|^3. \quad (15b)$$

Figure 9 gives a plot of Y versus X using such simplifications. In constructing this plot the PE's were computed from observed σ_t values at stations in the outer-shelf regions where h = 30–40 m and then averaged over the number of stations. For each PE value so obtained at time t, the wind stress and wind work were back-averaged from $t - \Delta t$ to t, where Δt = 3 days. Values of Δt = 2 and 4 days were also tried without significantly affecting the results. From O86 we estimate that $\alpha Q/C_{pw}$ and $\beta S_0 E_v$ over the shelf-break region are about 5×10^{-5} kg (m^2 s)$^{-1}$ and 5×10^{-6} kg (m^2 s)$^{-1}$ respectively. Thus, the contribution due to $(E_v - P_r)$ in C_1 can be neglected. The solid line in Fig. 10 gives values of the surface flux contribution to C_1 due to sensible heat flux [i.e., $(gh/2)(\alpha Q_{\text{sensible}}/C_{pw})/M$] calculated by using the measured air temperature at SNLT (Fig. 3) for the ten observational periods. This shows that, since contribution from the latent heat loss is of the order of that from sensible heat loss (O86), the surface flux contribution to C_1 is about 10^{-3}. Van Aken (1986) gives $C_{0a} \approx C_{0b} \approx 10^{-3}$ and assuming that $C_a \approx C_b$, $|\mathbf{u}_T| \approx 0.5$ m s^{-1} and $|\mathbf{u}_a| \approx 10$ m s^{-1}, the contribution to C_1 from the tidal work term is about 10^{-4}. These estimates give C_1 in (15b) of the order of 10^{-3}, and with $C_2 \approx 3.3 \times 10^{-3}$, which corresponds to an averaged (for all of the ten cruises) σ_t change of -0.5 kg m^{-3} from about the 30 m isobath to the shelf break,

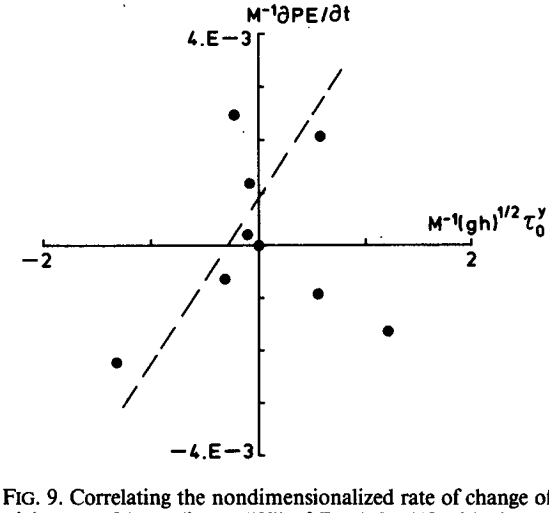

FIG. 9. Correlating the nondimensionalized rate of change of potential energy [the ordinate, "Y" of Eq. (15a, b)] with the nondimensionalized along-shelf wind stress [abscissa, "X" of Eq. (15a, b)]. Solid dots are values (one near the origin) calculated from observed hydrographies. The dashed line is an estimated "fit" obtained as explained in the text.

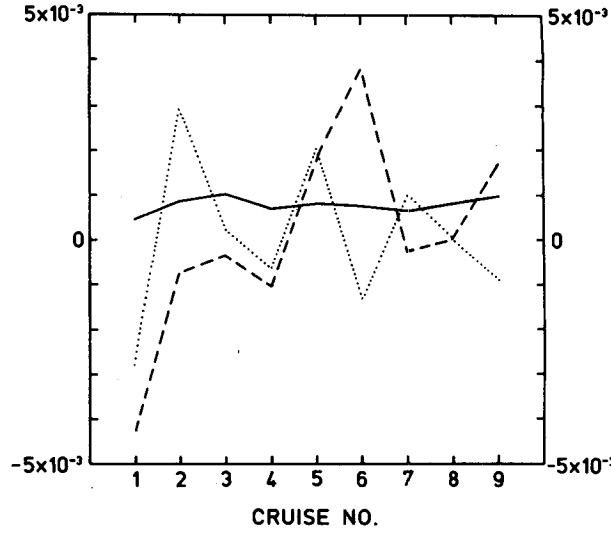

FIG. 10. A plot of estimated sensible heat flux (solid), the wind-induced advection term [dashed, C_2X in Eq. (15a, b)] and the rate of change of potential energy [dotted, Y in Eq. (15a, b)], all nondimensionalized, for the ten observational cruises from 10–30 January 1986.

we have plotted in Fig. 9 the dashed line of slope C_2 passing through the point $X = 0$, $Y = C_1 \approx 10^{-3}$. These estimates are clearly very rough. We are not overly concerned, however, with obtaining more exact values of C_1 and C_2 as long as they have the correct order of magnitude and are consistent with the hydrographic data.

The data points show scatter, but one can nevertheless discern a trend along the theoretical (dashed) line which suggests wind-induced intrusion processes. Note, however, that condition (15) is only necessary but not sufficient for the detection of wind-induced intrusion processes. Shoreward intrusion by Gulf Stream meanders and eddies can occur at the same instant as the wind-induced event, which may give one a false impression that wind-induced motion is predominant. Nevertheless, such occasion is relatively rare and one can usually differentiate between the two forcings. For example, the two points in the lower right-hand quadrant in Fig. 9 are clearly not wind related. They correspond to 22 and 30 January, when winds during the preceding 3–4 days were either offshore or northward. According to (15), these conditions favor positive Ys. The observed negative Ys shown in Fig. 9 suggest therefore that these intrusion processes were probably induced by Gulf Stream meanders (see Figs. 4g, 6g and 4k, 6j).

Finally, to assess the time dependency of surface flux terms [the last term of C_1 in (15b)], we note that the (nondimensionalized) sensible heat flux contribution to "Q" in (15b) as shown in Fig. 10 (which for comparison also includes plots of Y and C_2X) is relatively constant over the time period being examined. This supports the presumption that C_1 is a constant in (15).

5. Transient shelf-break upwelling

Present observations and numerical calculations in O86 show that transient upwelling occurs over the shelf-break/slope region near the end of southward wind events (Figs. 4b, 6b and 7). The first-order dynamics of this response can be explained by the following simple model.

We assume that the water is well mixed before the upwelling event. This is reasonable, since prior to the upstream wind event, observation shows a deep mixed layer [O(100 m)] over the shelf break and slope (Fig. 4a). Again neglecting any alongstream variabilities, we consider, therefore, an initially steady (or quasi-steady) Gulf Stream geostrophically maintained by a cross-stream sea level gradient:

$$fv_0 = g(d\eta_0/dx) \tag{16a}$$

$$u_0 = 0 \tag{16b}$$

where u_0 and $v_0(x)$ are vertically averaged velocity components in the x and y directions respectively, and $\eta_0(x)$ is the sea level elevation.

We now consider wind-induced perturbations governed by the following set of linear equations

$$fv_1 = g\eta_{1x} \tag{17a}$$

$$v_{1t} = (\tau_0{}^y - rv_{1b})/H \tag{17b}$$

in which subscripts "1" denote perturbation quantities, subscripts "x" and "t" denote partial derivatives, $H(x)$ is the depth of water and the bottom stress is modeled by rv_{1b}, where r is a bottom friction coefficient of $O(10^{-3}$ m s$^{-1})$, v_{1b} is the near-bottom alongstream perturbation velocity and for convenience of notation we have set $\tau_0{}^y$ to be the *kinematic* wind stress. If we replace v_{1b} with v_1, which implicitly assumes a zero phase lag between the near-surface and near-bottom currents, and perhaps also a corresponding reduction in r, we obtain for the perturbation vorticity, $\zeta_1 = v_{1x}$:

$$\zeta_{1t} = -(\tau_0{}^y - rv_1)(dH/dx)/H^2 - (r/H)\zeta_1. \tag{18}$$

For $dH/dx > 0$, Eq. 18 shows an increase in cyclonic vorticity ζ_1 resulting from southward wind stress ($\tau_0{}^y < 0$). The vorticity ζ_1 increases because the western side of the Gulf Stream front, being in shallower water, responds faster to winds than water columns further eastward. Associated with this increase in cyclonic vorticity is the observed upward-doming of isopycnals.

The solutions to (17b) and (18) for a wind-stress forcing of the form

$$\tau_0{}^y(t) = -[H_v(t) - H_v(t - t_0)], \tag{19}$$

where $H_v(t) = 0$ for $t \leq 0$ and $H_v(t) = 1$ for $t > 0$, are

$$v_1(x,t) = -[1 - e^{-(t/H)}] - H_v(t - t_0)[e^{-(t-t_0)/H} - 1] \tag{20a}$$

$$\zeta_1(x,t) = (H_x/H^2)[te^{-(t/H)} - H_v(t - t_0)(t - t_0)e^{-(t-t_0)/H}]. \tag{20b}$$

Here we have nondimensionalized x by L_0, the width of the upwelling region (~10 km); H by H_0 (~100 m); t and t_0 by (H_0/r); $\tau_0{}^y$ by τ_0, the wind-stress amplitude; v_1 by τ_0/r; and ζ_1 by $\tau_0/(rL_0)$. The duration time period of the wind is t_0.

With $x = 0$ positioned at the center of the upwelling region, and with

$$H(x) = 1 + x, \quad -\tfrac{1}{2} \leq x \leq \tfrac{1}{2}, \tag{21}$$

v_1 and ζ_1 at $x = 0$ are plotted in Fig. 11 for various values of t_0. For $r = 3.7 \times 10^{-4}$ m s^{-1} (Fig. 11a), as given in Schwing et al. (1985) for the continental shelf regions off Georgia and Carolina, one unit of t is approximately 3 days for $H_0 \approx 100$ m isobath, over which observations show upwelling. Other values of r correspond simply to a stretching and shrinking of the t axis. For example, Fig. 11b shows solutions for $r = 10^{-3}$ m s^{-1}, which correspond to approximately 1 day for one unit of t.

The time t_m for maximum vorticity when upward doming of isopycnals at $x = 0$ should be most evident is, from (20b),

$$t_m = \begin{cases} 1, & \text{for } 1 \leq t_0 \\ t_0, & \text{for } t_0 < 1 \end{cases} \tag{22}$$

so that solutions in Fig. 11a more nearly correspond to the observed upwelling (Fig. 4b) that followed an intense southward wind lasting for about 3 days (8–11 January).

Using a (kinematic) wind stress of 2×10^{-4} m^2 s^{-2}, a friction coefficient $r = 3.7 \times 10^{-4}$ m s^{-1} and depth = 100 m yields an estimate of about -3×10^{-3} s^{-1} for vertical shear on the western side of the upwelling dome. Therefore, from the thermal wind relation

$$\rho_x/\rho_0 = (-f/g)v_z, \tag{23}$$

we obtain $\delta\rho \approx 0.2$ kg m^{-3} across the upwelling dome. This is comparable to the value observed in Fig. 6b.

Finally, using the aforementioned values, we estimate a maximum perturbation (dimensional) vorticity of approximately 2.5×10^{-5} s^{-1}. This is a rather high value, comparable to the perturbation vorticity induced by Gulf Stream meanders (Brooks and Bane, 1983). One wonders if the wind-induced perturbation vorticity can be identified from observations. The time scale for the decay of wind-induced perturbations is about 1 day (Fig. 11 and Figs. 4b, c). Thus, it is likely that 40-hour low-passed data cannot be used to identify perturbations due to short-duration wind events. For t_0 (dimensional) $\geq$ 3 days, however, the vorticity maxima last longer and one may be able to identify their effects by direct observation.

6. Discussion

The correlation formula, Eq. (15), and the data analysis shown in Fig. 9 are fairly consistent with what

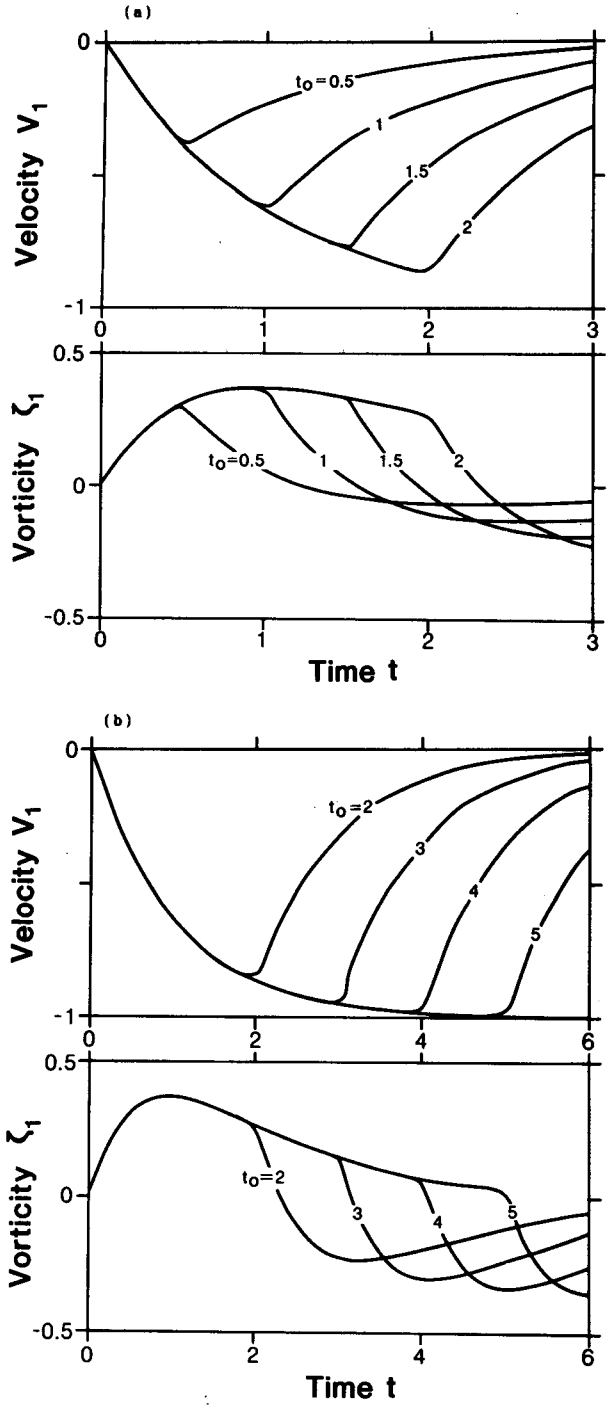

FIG. 11. Plots of the model's nondimensionalized along-stream perturbation velocity v_1 and vorticity ζ_1 at the center of the upwelling region, as functions of a nondimensionalized time t, for various duration times t_0 of southward wind stresses. The bottom friction coefficients r are (a) $r = 3.7 \times 10^{-4}$ m s^{-1} and (b) $r = 10^{-3}$ m s^{-1}.

we perceive as the role played by wind-induced horizontal advection, vertical mixing, and cross-shelf density gradients in determining shoreward intrusions of Gulf Stream water across the shelf break. We must caution, however, that the analysis is based on a few scattered observational data and a more thorough analysis will have to employ continuous time series from current meters and CTDs. These were deployed during GALE at the shelf break and outer continental shelf regions by Dr. T. Lee and coworkers at the University of Miami (Williams and Lee, 1986). Such a detailed analysis is currently being planned and we shall report the results in a separate paper. Blanton et al. (1987) used Eq. (15) to attempt a correlation of CTDs and wind data in the nearshore frontal zone off the coast of Georgia from 17 April through 16 June 1985. Except for reversals in the current directions and the presence of a shoreline, this nearshore strip of a freshwater-induced buoyant water mass is in some respects similar to the warm strip of water on the outer continental shelf just inshore of the shelf break. Excluding effects of Gulf Stream meander-induced intrusions in the outer continental shelf and neglecting effects of localized river plumes nearshore, the state of stratification of water columns in both systems is primarily governed by cross-frontal advection in the presence of cross-frontal density gradients, buoyancy inputs across the air–sea interface and mixing by winds and tides. Since wind-induced advection is expected to be significant nearshore, one expects that Eq. (15) gives good correlation with data. Blanton et al. (1987) found a fairly good correlation for the first half of their data series (17 April–16 May) and poor correlation for the second half (17 May–16 June), when the shelf water became almost a two-layer system. In this latter case, the idea that vertical stratification is affected by wind-induced advection in the presence of cross-shelf density gradients, upon which Eq. (15) depends, is no longer applicable.

As stated previously, the correlation analysis based on Eq. (15) alone is not sufficient to separate out wind-induced and Gulf Stream meander-related shoreward intrusion events. One can generally confirm a meander-related intrusion event from hydrographies, however. For example, the surface water found on the outer continental shelf on 30 January (Figs. 4k and 6j) suggests the cross-shelf structure of a warm filament (compare Figs. 6i, j with 6a, b) which trails behind the northward-propagating cyclone produced by instability of the meandering Stream (Brooks and Bane, 1983; Lee and Atkinson, 1983; Oey, 1987). While the sequence of dynamical events which leads to the two intrusion processes are necessarily different, our present data and Atkinson's (1977) data suggest a common feature: that is, these wintertime intrusions occur across the shelf break in the upper layer (i.e., overriding intrusions), as opposed to summertime intrusions which generally occur in the lower layer (bottom intrusions). Theoretical considerations (Oey, unpublished results) suggest that during winter the shelf-break front which extends the "western wall" of the Gulf Stream front over the shelf break acts as a dynamic barrier to any bottom intrusion. This is because in the presence of a

negative offshore density gradient across the shelf break, perturbations which tend to tilt the (shelf break) front clockwise (in the cross-frontal plane looking "northward", and hence induce "bottom" intrusions) would induce such intense vertical mixing as to prevent any further cross-shelf movement of the front. This view is consistent with Atkinson's (1977) results that "overriding" shoreward intrusions of Gulf Stream water are predominant during winter.

If "bottom" intrusions of Gulf Stream water into the continental shelf proper are unlikely, why is it then that one often finds during winter in the mid- to outer-shelf regions high algae populations (Paffenhofer, 1986, private communication), which presumably feed on organic matter formed in part by the upwellings of nutrient-rich Gulf Stream water from below the mixed layer? The results presented here and in O86 offer a possible explanation. Transient upwellings over the shelf break of nutrient-rich, subsurface Gulf Stream water accompany shoreward intrusion events as described in section 5. The time taken by a water parcel to be upwelled and subsequently transported shoreward onto the continental shelf is of the order of a few days (section 2), which is ample time for growth of phytoplankton seeded by subsurface nutrients to form chlorophyll (Ishizaka et al., 1983). Thus, the upper 100 m or so of the Gulf Stream just seaward of the shelf break serves as a storage of nutrient-rich water, which is periodically being replenished from below, and at the same time is ready to be flushed shoreward by shoreward intrusion events of periods which coincide with the "weather" cycles (~3–10 days) and/or the Gulf Stream meander cycles (~8 days).

7. Conclusions

Repeated hydrographic measurements taken along a cross-shelf transect from Charleston, South Carolina, (32.8°N, 80°W) to the shelf break and continental slope regions (31.8°N, 78.6°W) over the Gulf Stream from 10 to 30 January 1986 support the hypotheses that during winter

1) the "western wall" of Gulf Stream front surfaces at the shelf break to form a shelf-break front, which separates warm upper Gulf Stream water from cooler shelf water; and

2) perturbations which tilt the front counterclockwise (in the cross-frontal plane looking "northward"), induced by either southward winds or/and Gulf Stream meanders, produce a shoreward transport of warm surface water. The intruded warm water mixes with the cooler continental shelf water to form a continental shelf front with negative offshore density gradient.

We have formulated simple models which encompass the gross features of Oey's (1986) more extensive numerical model. The models were used to describe transient shelf-break upwelling following a southward wind event and also to correlate alongstream wind forcings with the observed rate of change of potential energy of water columns just inshore of the shelf break. The correlation analysis attempts to describe the shoreward intrusion processes. The correlation fit was fairly good. In conjunction with hydrography measurements, model correlation could be used to differentiate between Gulf Stream meander-related and wind-induced intrusion processes. Our analysis shows that during winter, wind-induced shoreward intrusions of upper Gulf Stream water are prominent features of the Gulf Stream–continental shelf interaction processes.

Acknowledgments. Thanks to Chisato Mizutani for typing the manuscript, to Tom Berger and Bill Chandler for providing the hydrographic contour plots, and to Kathy Bush for commenting on the first draft. This research has been supported by the National Science Foundation under Grant OCE-85 16129.

REFERENCES

Atkinson, L. P., 1977: Modes of Gulf Stream intrusions into the South Atlantic Bight shelf waters. *Geophys. Res. Lett.*, **4**, 583–586.

——, W. S. Chandler, T. J. Berger and W. M. Dunstan, 1986: Preliminary Cruise Report of the Research Vessel ENDEAVOR Cruise EN-140, part of the GALE Project. Dept. of Oceanogr. Rep., Old Dominion University, 15 pp.

Blanton, J. O., L.-Y. Oey, J. Amft, T. N. Lee and K. Bush, 1987: Advection of momentum and buoyancy in a coastal frontal zone. Submitted to *J. Phys. Oceanogr.*

Brooks, D. A., and J. M. Bane, 1983: Gulf Stream meanders off North Carolina during winter and summer 1979. *J. Geophys. Res.*, **88**, 4633–4650.

Gill, A. E., 1982: *Atmosphere–Ocean Dynamics.* Academic Press, 662 pp.

Ishizaka, J., M. Takahashi and S. Ichimura, 1983: Evaluation of coastal upwelling effects on phytoplankton growth by simulated culture experiments. *Mar. Biol.*, **76**, 271–278.

Lee, T. N., and L. P. Atkinson, 1983: Low-frequency current and temperature variability from Gulf Stream frontal eddies and atmospheric forcing along the southeast U.S. outer continental shelf. *J. Geophys. Res.*, **88**, 4541–4567.

Mellor, G. L., and T. Yamada, 1974: A hierarchy of turbulence closure models for planetary boundary layers. *J. Atmos. Sci.*, **31**, 1791–1806.

Oey, L.-Y., 1984: On steady salinity distribution and circulation in partially mixed and well-mixed estuaries. *J. Phys. Oceanogr.*, **14**, 629–645.

——, 1986: The formation and maintenance of density fronts on U.S. southeastern continental shelf during winter. *J. Phys. Oceanogr.*, **16**, 1121–1135.

——, 1987: A model of Gulf Stream frontal instabilities, meanders and eddies along the continental slope. *J. Phys. Oceanogr.*, in press.

Schwing, F. B., L.-Y. Oey and J. O. Blanton, 1985: Frictional response of continental shelf water to local wind forcing. *J. Phys. Oceanogr.*, **15**, 1733–1746.

Simpson, J. H., and J. R. Hunter, 1974: Fronts in the Irish Sea. *Nature*, **250**, 404–406.

van Aken, H. M., 1986: The onset of seasonal stratification in shelf seas due to differential advection in the presence of a salinity gradient. *Cont. Shelf Res.*, **5**, 475–485.

Williams, E., and T. N. Lee, 1986: GALE, 1986, Coastal Ocean Response Experiment Preliminary Data Report, Rosenstiel School of Marine and Atmospheric Science, University of Miami. 45 pp.